Helical axis and modeling of the upper cervical spine

An in vitro analysis

Dugailly P.-M. [*†§], Sobczak S. [*], Sholukha V. [*], Klein P. [§], Van Sint Jan S. [*], Salvia P. [*], Feipel V. [*], Rooze M. [*]

[*] Dept. of Anatomy, [†] Dept. of Physiotherapy (Hôpital Erasme), [§] Research Unit for Manual Therapies

Université Libre de Bruxelles

Brussels, Belgium

pdugaill@ulb.ac.be

***Abstract*—Registration of 3D anatomical model and kinematics data is reported to be an accurate method to provide 3D joint simulation. We applied this approach to upper cervical spine kinematics analysis. Although partially confirming previous results, helical axis computation showed variations of motion patterns dependent on movement, level and specimen.**

Keywords: Upper cervical spine, kinematics, helical axis, modelling, simulation

I. Introduction

Previous studies investigating cervical kinematics mainly used biplanar analysis for describing joint displacement and motion axis location [1,2]. Several studies have suggested 3D methods using helical axis computation for analyzing kinematics of joints such as the knee, wrist, foot and lower cervical spine [3,4,5,6]. In this way, results clearly document that the helical axis (HA) provides extended data concerning segmental coupled motion during global movement. Presently, fundamental and clinical research applications combining *in vitro* or *in vivo* kinematic data with medical imaging data focusing on musculoskeletal functions of the human body are emphasized [7,8]. Different procedures have already been validated and provide accuracy for measuring 3D kinematics [8]. According to these authors, registration of morphological and kinematics data supplies consistent biomechanical information. The aims of this study were to develop a standardized protocol for analyzing upper cervical spine (UCS) kinematics and for creating 3D modeling and simulation using registration of individual kinematics and anatomical data.

II. Methods

Ten unembalmed human specimens were sampled. Dissection of superficial soft tissues was realized by two experimented operators to access the UCS and its connected anatomical structures such as ligaments, suboccipital muscles and fascias. All these structures were kept intact. The lower cervical segments (below C3) and their related soft tissues were removed as well as the mandible and anterior viscera of the neck.

A. Instrumentation and experimental set-up

To assess UCS kinematics, a 3-D caliper (Faro Arm, B06/Rev 18; Faro Technologies Inc; USA) was used for computing the spatial position of bony segments in different positions of flexion-extension (FE) and axial rotation (AR). Each bone was identified by technical markers (TM) consisting of aluminum balls (diameter: 4mm). Four balls were fixed on the occipital bone (C0), 4 on the atlas (C1) and 3 on the axis (C2).

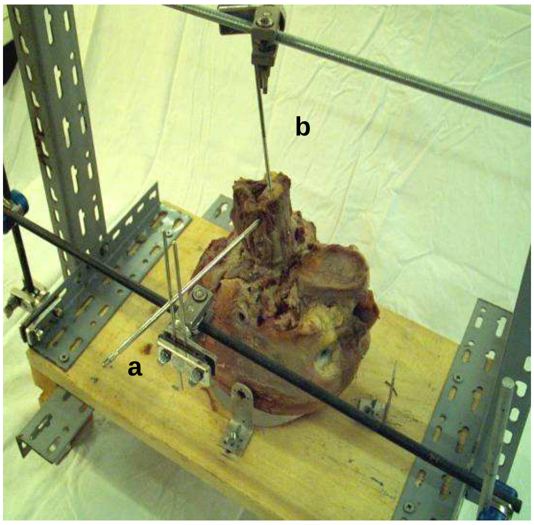

Figure 1. Experimental set-up

Motion of cervical vertebrae was applied by two metallic drills fixed at the third cervical segment, one through the transverse processes (a) and one vertically (b) through the vertebral body (fig.1). Stabilization of drills assured application of pure single movement in the sagittal or horizontal plane. No external loading was applied to the vertebral segments. For each movement plane (horizontal and sagittal), 5 discrete positions were sampled through the full range of motion for measuring spatial location of each bone. In addition, coordinates of anatomical markers (AM) (fig.2) were obtained in *neutral position* using the single point digitizing mode. Then, the specimen was firmly fixed in this position and frozen for CT imaging.

B. Imaging and segmentation

Imaging acquisition was performed using a computed tomography system (Siemens SOMATOM, helical mode, reconstruction: slice thickness = 0.5mm, interslice spacing = 1mm). The 3D reconstruction was carried out for each bone separately using segmentation software (Amira 3.0, San Diego, CA, USA) to define accurate contours of the bony structures. From the same CT dataset, a second image dataset was obtained including the technical markers. From these two datasets, all surface files were stored in virtual reality modeling language (VRML) prior to simulation processing.

C. Kinematics computing and analysis

To compute spatial bone motion, each segment's position and orientation were determined in its local reference coordinate system (fig.2). After extracting angular data from the orientation matrix [14], kinematics data analysis was carried out in a global coordinate system set on C2. To provide motion simulation of each 3D geometric model, a validated registration method [8] was processed for combining kinematics and imaging data. This procedure was performed using an integrated computer graphic environment (Data Manager, Multimod Project IST-2000-28377)

In addition, HA parameters were computed to indicate HA orientation and location in the local reference systems such as C1 and C2 for C0-C1 and for C1-C2 respectively. HA data were included into each 3D model to represent HA evolution during simulation. Inclination of the mean HA (MHA) was also computed for each specimen in different reference planes (frontal, sagittal and horizontal).

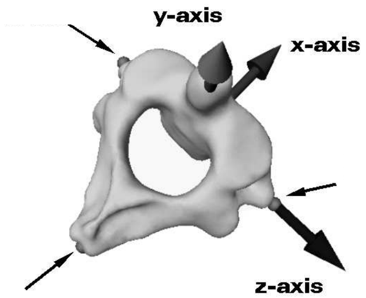

Figure 2. Local reference system and orientation of x,y and z axes with respect to anatomical markers (dots).

III. RESULTS

A. Global motion analysis

Average values for maximal amplitudes are found in table 1 for C0-C1, C1-C2 levels and for C0 with respect to C2 for FE and AR. As expected, principal motion was observed around y-axis and z-axis for AR and FE respectively.

For AR, a larger range of motion was clearly demonstrated for C1-C2 as compared to C0-C1 and small coupling motions were displaying. In general, heterolateral bending occurred at C0-C1 and irrelevant motion was observed in the sagittal plane at both levels.

For FE, principal movement around the z-axis was found to be slightly larger for C0-C1 than for C1-C2. Lateral bending or AR was demonstrated neither at C0-C1 nor C1-C2 nor between C0 and C2.

For the entire sample, global range of motion of C0-C2 was between 38 and 74 and between 25 and 49 degrees for AR and FE respectively.

TABLE 1.

	AXIAL ROTATION		
	C0-C1	C1-C2	C0-C2
x	2,3 (2,0)	0,5 (5,2)	2,6 (4,4)
y	5,0 (3,4)	46,1 (12,5)	51,1 (13,5)
z	0,8 (3,5)	-0,7 (5,3)	0,4 (2,7)
	FLEXION - EXTENSION		
	C0-C1	C1-C2	C0-C2
x	-0,1 (1,3)	0,7 (1,6)	0,9 (2,6)
y	-1,7 (3,3)	1,9 (4,5)	0,3 (5,8)
z	-19,1 (5,8)	-14,3 (3,3)	-33,4 (5,7)

Global amplitudes: average (SD) in degrees around x,y, z axis.

For FE and AR, relatively similar motion patterns were observed for C0-C1 and C1-C2 in each specimen. However, exceptions were noted for some cases. Concerning coupled movement comparable patterns were also shown between specimens at each spinal level.

B. Helical axis location

Analysis of HA demonstrated different location and orientation depending on the principal motion, the vertebral level and the specimen. HA location and orientation were more variable at C1-C2 for FE although mobility was only slightly lower to the C0-C1 level (fig.3).

Average values of (and standard deviations) MHA inclination to the respective planes are shown in table 2.

TABLE 2.

	frontal	sagittal	horizontal
AR (at C1-C2)	-1.9 (12.2)	-1.5 (7.8)	
FE (at C0-C1)	2.4 (7.3)		0.4 (6.8)

During FE, HAs were located at the level of the occipital condyles and displayed little displacement and orientation variation for most specimens. During AR, helical axis position was found to be at the level of the dens of C2. This location was relatively constant and its orientation corresponded mostly to the direction of the dens for all specimens (fig.4).

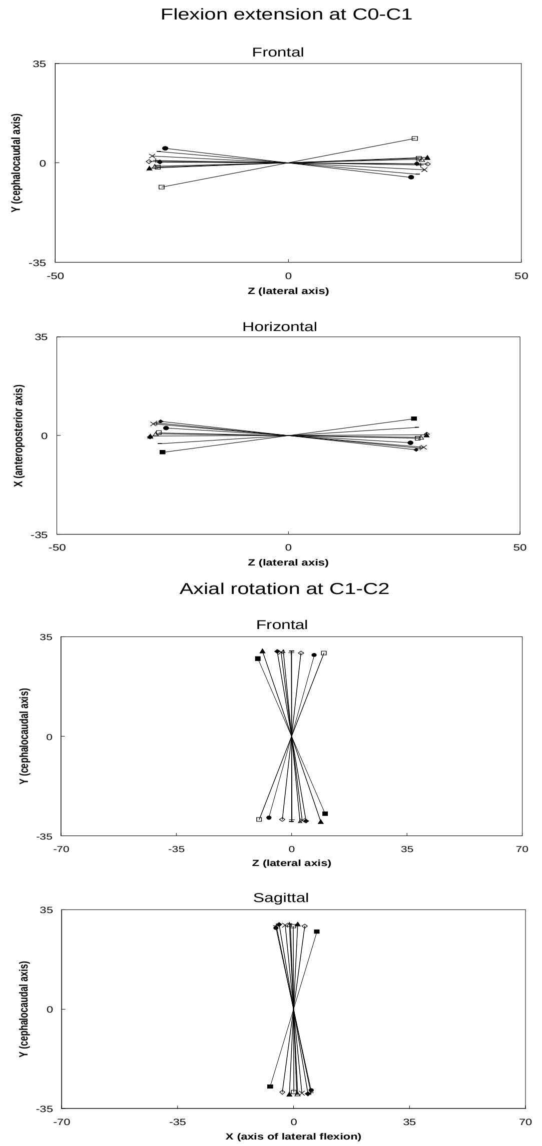

Figure 3. MHA orientation in the frontal and horizontal planes during FE and AR at C0-C1 and C1-C2 (10 specimens).

IV. DISCUSSION

The objectives of this study were to develop a protocol to investigate UCS kinematics based on previously validated procedures [8]. The findings of this study are innovative related to the computation of HA and modeling of UCS during movement.

The most recent studies on UCS *in vivo* and *in vitro* kinematics reported larger FE and AR ranges of motion compared to the present study [2,9]. However, our findings are in agreement with Kettler et al. [10] and Chin et al. [11].

During AR, coupled movements were observed in the sagittal and frontal planes. These coupling motions are well described for the UCS [7,11,12]. In general, lateral bending was opposite to the rotation with slight extension occurring at C0-C1 whereas flexion was present at C1-C2. However, large variation was observed. In our study coupled flexion movement was very small and large variation was observed for the whole sample.

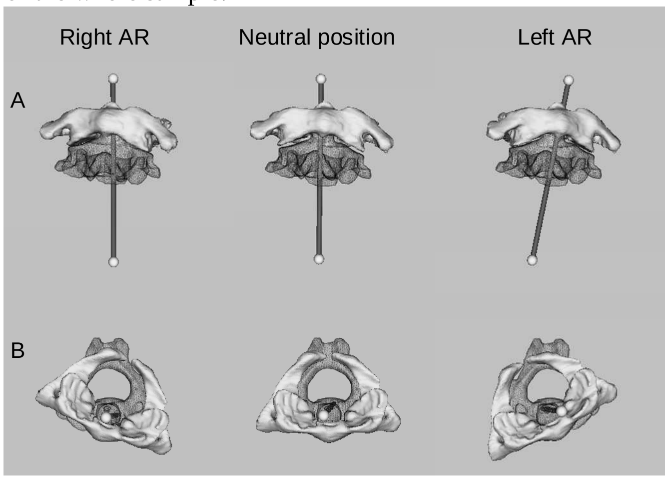

Figure 4. Illustration of one UCS model (atlantoaxial level) and HA location for three different discrete positions of axial rotation.

In general, analysis of motion patterns demonstrated that specimens displayed similar patterns for AR as well as FE movement. Higher similarity was demonstrated around the principal y- and z-axes of movement, respectively. Different patterns were more frequent during FE, where coupled motions were observed around the y-axis in some cases.

Estimation of the HA is poorly reported for cervical segments such as the occipitoatlantoaxial complex. Studies [9,12,13] have described an approximated instantaneous axis of rotation (IAR) located at the level of the axis dens during C1-C2 AR. According to these authors this axis should shift in direction of the lateral mass of the atlas opposite to the rotation direction. In our study, HA analysis showed a relatively constant location and orientation during AR at C1-C2 level (i.e. no lateral migration) as well as during FE at the C0-C1 level. For FE localization of IAR for C0-C1 was mostly reported at the level of the occipital condyles with different cranial and dorsal situations depending on the studies [7,9]. In our 3D analysis, estimation of HA location was in agreement with these previous studies but orientation variation was also demonstrated. On the opposite, larger HA location and orientation changes were observed for C1-C2 FE and C0-C1 AR. We believe that this observation should be also related to several factors such as degenerative aspects, congruence and orientation of joints, *in vitro* conditions and soft tissue stiffness, that might induce small accessory patterns of movement. In this way, HA estimation could provide consistent information to investigate 3D kinematics related to different anatomical aspects of cervical joints [15]. The latter consideration, as previously mentioned, is currently lacking in the biomechanics of the cervical spine.

In an attempt to compare HA data between specimens, inclination of HA was computed in different planes. This method was previously used for the ankle and subtalar joints [6].

Using a standardized procedure, this study focussed on registration methods of kinematics and imaging data to obtain 3D anatomical models and movement simulation of the upper cervical segments. Computed kinematics and helical axis data were integrated to UCS 3D models to provide visualisation of anatomical segment motion, joint behaviour and HA pattern during flexion extension and axial rotation.

These preliminary results need to be extended by assessing different loading conditions as well as continuous movement application and resulting kinematics data. In addition, this method could be the starting point for the development of future in-vivo applications on asymptomatic subjects or patients.

REFERENCES

[1] Fuss FK. Sagittal kinematics of the cervical spine--how constant are the motor axes? Acta Anat 1991;141:93-6.

[2] van Mameren H, Sanches H, Beursgens J, Drukker J. Cervical spine motion in the sagittal plane. II. Position of segmental averaged instantaneous centers of rotation: a cineradiographic study. Spine 1992;17:467-74.

[3] Salvia P, Woestyn L, David JH, Feipel V, Van S, Jan S, Klein P, Rooze M. Analysis of helical axes, pivot and envelope in active wrist circumduction. Clin Biomech 2000;15:103-11.

[4] Woltring HJ, Long K, Osterbauer PJ, Fuhr AW. Instantaneous helical axis estimation from 3-D video data in neck kinematics for whiplash diagnostics. J Biomech 1994;27:1415-32.

[5] Leardini A. Geometry and mechanics of the human ankle complex, and ankle prosthesis design. PhD thesis, University of Oxford 2000

[6] de Lange A. A kinematic of the human wrist joint. Ph. D. thesis, Faculty of Dentistry, Nijmegen University, The Netherlands (ISBN 90-9001762-3).

[7] Ishii T, Mukai Y, Hosono N, Sakaura H, Nakajima Y, Sato Y, Sugamoto K, Yoshikawa H. Kinematics of the upper cervical spine in rotation: in vivo three-dimensional analysis. Spine 2004;29: E139-144.

[8] Van Sint Jan S, Salvia P, Hilal I, Sholukha V, Rooze M, Clapworthy G. Registration of 6-DOFs electrogoniometry and CT medical imaging for 3D joint modeling. J Biomech 2002;35:1475-84.

[9] White AA, Panjabi MM. Clinical Biomechanics of the Spine. Philadelphia, J.B. Lippinscott Company, 1978.

[10] Kettler A, Hartwig E, Schultheiss M, Claes L, Wilke HJ. Mechanically simulated muscle forces strongly stabilize intact and injured upper cervical spine specimens. J Biomech 2002;35:339-46.

[11] Chin KH, Tan KW, Goh JCH, Toh SL, Lee VSP. Flexibility testing of the human upper cervical spine under continuous loading and unloading. Summer Bioengineering Conference 2003; Key Biscayne Florida.

[12] Iai H, Moriya H, Goto S, Takahashi K, Yamagata M, Tamaki T. Three-dimensional motion analysis of the upper cervical spine during axial rotation. Spine 1993;18:2388-92.

[13] Pfirrmann CWA, Binkert CA, Zanetti M, Boos N, Hodler J. Functional MR imaging of the craniocervical junction. Correlation with alar ligaments and occipito-atlantoaxial joint morphology: a study in 50 asymptomatic subjects. Schweiz Med Wochenschr 2000;130:645-651.

[14] Cappozzo A, Catani F, Della Croce U, Leardini A. Position and orientation in space of bones during movement: anatomical frame definition and determination. Clin Biomech 1995;10:171-178.

[15] Roche CJ, King SJ, Dangerfield PH, Carty HM. The atlanto-axial joint: physiological range of rotation on MRI and CT. Clin Radiol 2002;57:103-8.